COMPUTATIONAL MODELLING OF BEHAVIOUR OF SOFT BIOLOGICAL TISSUES

J.Burša, R. Lebiš and P. Ryšavý

* Brno University of Technology, FME, ISMBM, Technická 2, 61669 Brno, CZ

bursa@fme.vutbr.cz

Abstract: The paper deals with computational modelling of mechanical behaviour of soft tissues in arterial wall. Three computational models are presented. Model No. 1 models abdominal aortic aneurysms (AAA) at the level of a multilayer aortic wall structure with hyperelastic isotropic material properties of the individual layers. The extreme principal stress in the AAA is evaluated and compared with the stress in an intact aorta. The ratio of these stresses should be used in the evaluation of AAA rupture risk. Model No. 2 models an individual smooth muscle cell (SMC) at the level of a homogeneous hyperelastic isotropic continuum. Parameters of the 5-parameter-Mooney-Rivlin constitutive model are identified from the tension test of the SMC. Model No.3 models tension and indentation tests of SMCs with taking the cell structure into account, with cytoskeleton represented by a simple tensegrity structure.

Introduction

The paper is focused on computational modelling of arteries and smooth muscle cells they are abounding with. The problems to be solved in this field were induced by the fact that artificial replacements began to be used in cardio-vascular surgery in several last decades. Vascular grafts used as replacements of partially or fully occluded arteries are examples of such replacements; furthermore, various supports are used more and more frequently in the vascular system (e.g. arterial stents). Also some sorts of surgical treatments based on mechanical principle bring similar, i.e. among others also biomechanical problems (e.g. angioplasty or resection of parts of arteries). A frequent use of these procedures requires a thorough knowledge on properties of all tissues and other materials in question. Remodelation of the tissues, i.e. adaptation of their structure to the changed conditions, is a typical response of the living tissues on the changed mechanical load; these processes tend to re-establish the original physiological state. Also atherosclerotic changes are stimulated by mechanical factors such as high blood pressure, endothelial damage etc. Since all of these processes start at the cellular level, models at various levels are created and solved, from the macroscopic level with only one or a few homogeneous layers throughout the arterial wall down to the microscopic level at which we modell mechanical behaviour of individual smooth muscle cells (SMCs).

Materials and Methods

The problems of stress-strain analysis of diseased or mechanically treated arteries, at both *macroscopic and microscopic levels*, are solved using computational modelling based on finite element method; in particular, the program system ANSYS is used in all of the presented computational models. At a *macroscopic level*, a model for stress-strain analysis of abdominal aortic aneurysms (AAA) is presented in the paper (further denoted as *model No. 1*). The extreme stress values in the wall of the AAA are compared with extreme values in the intact aorta. The ratio of these two values enables us to evaluate the risk of the AAA wall rupture better than the mere maximum AAA diameter, which is the only standard criterion used in clinical practice.

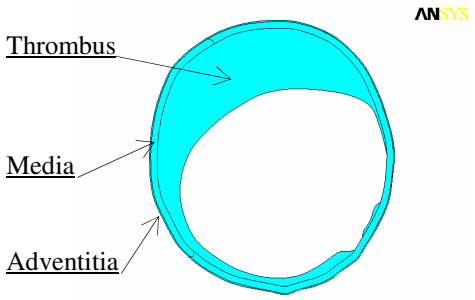

Figure 1: Segmented areas of the AAA cross section

Initial geometry of the 2D model is created on the basis of a CT image. The density comparison method was used for segmentation of CT images into various areas, corresponding to the basic tissue types (e.g. adventitia, media and thrombus). In particular, the maximum cross section of the AAA is divided into three planar areas (see fig. 1), which define the regions with different constitutive parameters of the material; sometimes even calcifications can be differentiated in the CT image as another one type of material. The computational model assumes homogeneous, isotropic, incompressible and nonlinear elastic behaviour of all materials in question (except of calcifications); in particular, Yeoh 3rd order hyperelastic constitutive model has been chosen. It is described by the following equation of the strain energy density function

ISSN: 1727-1983

$$W = \sum_{i=1}^{3} C_{i0} \left(I'_1 - 3 \right)^i \quad , \qquad (1)$$

where W is strain energy potential; I'_1 is the first deviatoric strain invariant; c_{i0} are material constants. The model is loaded by a stepwise increasing inner pressure up to 10 kPa and is solved under plane strain conditions to ensure zero axial deformations, what is (according to [1]) near the physiological conditions.

At a microscopic level, we model the mechanical behaviour of SMCs. Recently some results of tests carried out with isolated SMCs have been published; they can be simulated computationally to identify the constitutive relations of the cells or their components. We modelled the tests at two different levels: a homogeneous isotropic non-linear elastic material of the whole cell and the cell with its inner structure modelled as a tensegrity structure.

The tests carried out with individual SMCs and suitable for computational modelling are as follows:

Micropipette aspiration method [2] is based on aspiration of the cell into a micropipette (with inner diameter of several micrometers, i.e. smaller than SMC dimensions). It can be supposed that the aspiration is influenced mostly by the stiffness of the membrane with the cortex of cell, both modelled together by shell elements.

Indentation tests [3] have shown different stiffness in various parts of the cell; the central part (probably nucleus and its surroundings) is stiffer than peripheral parts of the cell. As the global shape of the cell does not change substantially during the test, a less pronounced influence of the deep cytoskeleton can be expected and the above difference is supposed to be caused by different properties of sarcoplasm in central and peripheral parts of the SMC. Under assumption of known properties of the cortex, parameters of sarcoplasm constitutive model in both parts of the model could be identified using computational simulation of these tests.

Tension tests [4] and *compression tests with microplates* [5] induce substantial global changes in the cell shape. As the endoskeleton appears to be the most important load-bearing structure of the SMC in this case, it is possible (when the cortex properties are known) to identify the constitutive parameters of this structure with known geometry and topology (as described e.g. in [6]).

A simple homogeneous model (further denoted as *model No. 2*) was solved as the first step in computational modelling of SMCs (of a contractile phenotype), with the aim of a more sophisticated evaluation of tension tests of SMCs published in [4]; the test results were presented there as dependencies between cell elongation and reaction force in a micropipette glued to the cell. The initial shape of the "in vitro" cultured cells was nearly spherical, so that there could not be a uniform stress state in the cell model and it is not correct to evaluate stresses and strains using any simple analytic formulas. The cells undergo large strain and the measured curves are nearly independent from the load direction. Therefore the cell material was supposed to be homogeneous isotropic with hyperelastic behaviour. The computational model enabled us to evaluate the stress-strain curves of this material and to identify the parameters of the chosen constitutive model in this way. Finally, we used Mooney-Rivlin five-parameter constitutive relation, describing the strain energy density function by the following formula:

$$W = a_1(i_1 - 3) + a_2(i_2 - 3) + a_3(i_1 - 3)^2 + a_4(i_1 - 3)(i_2 - 3) + a_5(i_2 - 3)^2 + \frac{\kappa}{2}(i_3 - 1)^2, \qquad (2)$$

where i_i are modified invariants of the right Cauchy-Green deformation tensor, κ denotes the bulk modulus and a_i are other material parameters (Mooney-Rivlin constants).

The parameters of the constitutive model were evaluated using an iterative approach. In the first step, the initial σ-ε curve was estimated and the parameters of the constitutive model evaluated from this curve were used in the model. Then the force-elongation curve obtained by computational simulation of the test was compared with the experimental one and the material parameters were modified with the aim to achieve a better agreement between the computed and experimental curves. This iteration process was repeated until a sufficient agreement between both curves was achieved (details see [7]).

Subsequently a more complex model (denoted further as *model No. 3*) of SMC was created, which comprehends structural parts of the cell substantial from the mechanical viewpoint, i.e. the following ones (see fig. 2):

- *Membrane skeleton* (cortex of cell) modelled together with the cell membrane as a shell on the cell outer surface.
- *Deep cytoskeleton* with geometry and topology based on a simple tensegrity structure. This structure consists of 6 struts (compression bearing elements) representing microtubuli and 24 cables (tension bearing elements) representing microfilaments.

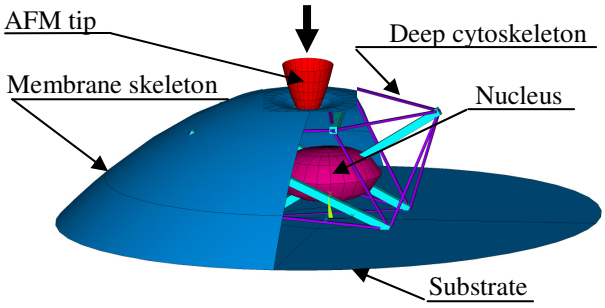

Fig.2: FE model (No.3) of indentation test

ISSN: 1727-1983

- Central part of the cell (*nucleus* and adjacent organelles, e.g. centrosome) modelled as an elastic continuum.
- Peripheral parts of *sarcoplasm* (except for nucleus and its surroundings) modelled as a very compliant elastic continuum.

In addition to the tension test (with the spherical initial geometry of the cell model), we tested the applicability of this computational model on modelling of the indentation tests, which is able to quantify the local stiffness in various points of the cell surface. The model of this test realized by atomic force microscopy (AFM) in [3] is shown in fig. 2. Model geometry corresponds to the real geometry of the cell cultivated on a rigid substrate.

Because of an unambiguous identification of elastic parameters of the model, all the materials of this model are supposed to be homogeneous, isotropic, linear elastic (elastic parameters and other details were published in [7]). The struts and cables of the tensegrity structure are modelled by 1D link elements, nucleus and sarcoplasm by 3D solid elements and membrane skeleton by shell elements. A low prestrain value was defined in the cytoskeleton cables (representing actomyosin contractile microfilaments) to stabilize the shape of the cell. The AFM tip stiffness is several orders higher than that of the cell so that the tip can be modelled as a rigid body to make the computation substantially less time-consuming.

The following *boundary conditions* were prescribed in the model: displacements of all nodes being in contact with the substrate are zero. Contact elements are used to model the contact between the AFM tip and the cell. The load is realized by vertical displacement of the AFM tip (see fig. 2), prescribed in its pilot node where the contact reaction force is also evaluated.

Results

Table 1: Maximum principle stresses and their ratio

blood pressure [kPa]	stress in the aneurysm [kPa]	stress in the intact aorta [kPa]	stress increase ratio in AAA
1	38	11	3,5
2	75	22	3,4
3	116	35	3,3
4	161	47	3,4
5	212	60	3,5
6	267	75	3,6
7	326	90	3,6
8	390	106	3,7
9	458	123	3,7
10	529	140	3,8

Model No.1 was loaded stepwise by the inner pressure, and we compare the maximum principal (circumferential in most cases) stress in the AAA with maximal values in the intact artery in the sequential load steps. An example of the stress distribution in the AAA wall is presented in figure 3. Table 1 presents the results in comparison with the values in an intact aorta.

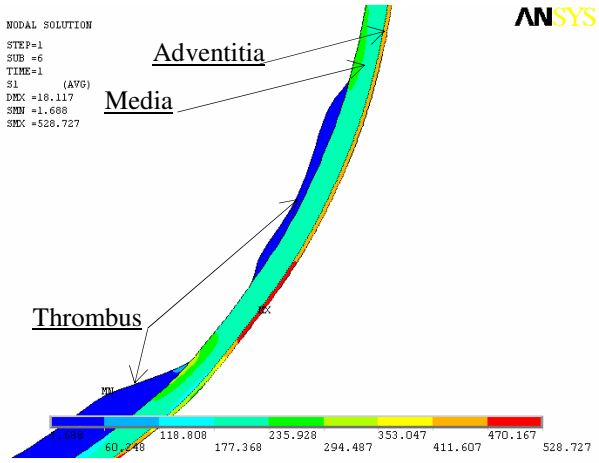

Figure 3: First principal stress distribution - detail of the AAA wall with trombus

The results of *model No.2* (SMC tension test) are presented in fig. 4 in the form of the resulting stress-strain curve of the material of the cell. The initial curve was computed by simple division of the measured force and elongation by the maximum cross section and diameter of the spherical cell, respectively. The resulting curve is input curve of the used Mooney-Rivlin material model (its constants see tab.2), which results in the force vs. elongation dependence nearly identical with the experimental one. More details about the procedure see [7].

Table 2: Mooney-Rivlin constants of a homogenized model of contractile SMC acc. to eq. (2)

a_1	a_2	a_3	a_4	a_5
-3,530	*3,862*	*-0,9833*	*3,1470*	*-0,4336*

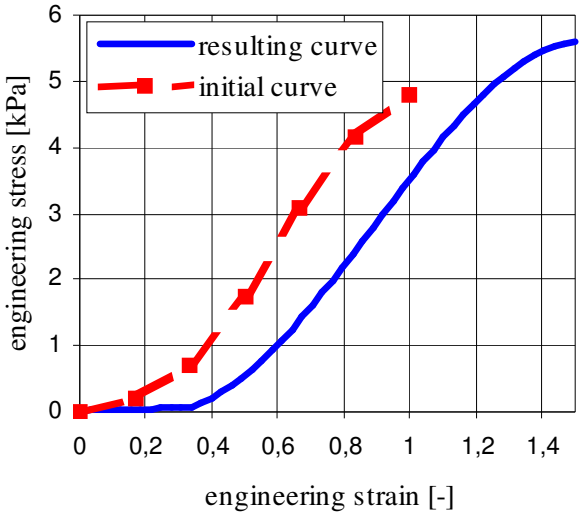

Figure 4: Initial and resulting stress-strain curves of a (homogeneous) smooth muscle cell

Model No.3 was tested in simulation of tension and indentation tests. Since the deep cytoskeleton is

ISSN: 1727-1983

modelled as a very simplified tensegrity structure, the stresses in cytoskeleton elements cannot be realistic. Illustrative resulting stresses in the sarcoplasm (incl. nucleus but excl. cytoskeleton) are presented in fig. 5.

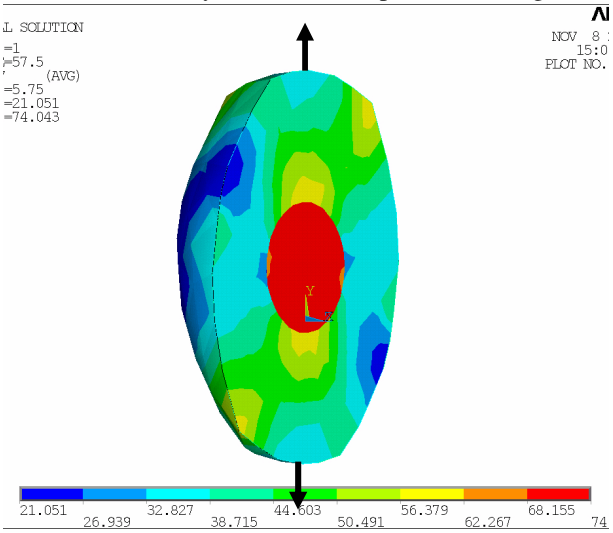

Figure 5: Illustrative Mises stress [kPa] distribution in SMC model No.3 during tension test

Results of computational simulation of the indentation tests using *model No.3* acc. to fig. 2 are evaluated in the form of the dependency of the reaction force in the pilot node on the indentation depth, i.e. in the way similar to the experiments in [3]. The simulation with the nominal values of elastic parameters (according to table 3) gave realistic results, being in accordance with the experiments (see fig.6).

Tab.3: Elastic parameters of cell components used in the computational model No.3

	Modulus of elasticity [kPa]	*Poisson's ratio [-]*
Micro-tubuli	4e5	*0,3*
Micro-filaments	5e5	*0,3*
Membrane skeleton	10	*0,3*
Cytoplasm	0,25	*0,45*
Nucleus	*1*	*0,3*

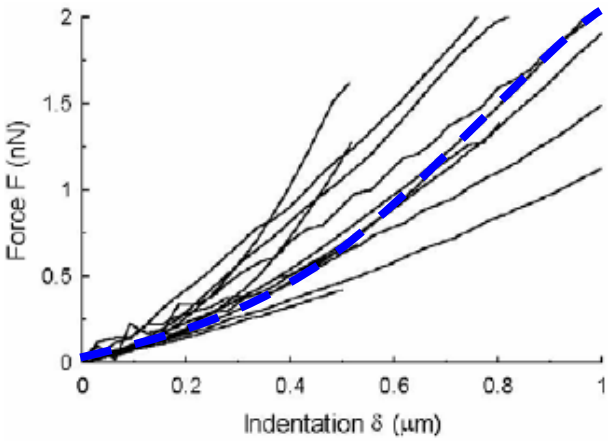

Figure 6: Comparison of the simulated curve (blue dashed line) with the experimental ones.

The elastic parameters were not determined by identification, because their number is too high to be identified from one type of experiment only. Therefore a sensitivity analysis was carried out by changing each of the elasticity moduli separately in the range of 50 – 200% of its nominal value; the influence of these changes was evaluated. Results of these simulations are presented in fig.7.

Discussion

The most significant problem of the *model No. 1* of the AAA is that we do not know which phase of the cardiac cycle the CT scan was made in. Therefore we are not able to determine the blood pressure in the moment of CT scanning. Therefore we evaluated the stress ratio between the AAA and intact aorta that is nearly independent of the blood pressure (see tab. 1). Then the stress ratio evaluated in this way should be a better criterion than the mere diameter of the AAA, as it is usual in clinical practice.

Even if the CT scanner is able to determine the phase of the cardiac cycle and, consequently, the blood pressure in this moment, we would not know the initial (unloaded and undistorted) geometry of the aorta and AAA, but only the shape under this load. The possibility very simple at first sight, namely loading of the model with the scanned geometry by a corresponding negative blood pressure to obtain the unloaded shape, fails because of shape instabilities (buckling). Therefore the only possibility of how to get an approximate unloaded shape is a homothetic transformation of the scanned shape with the ratio < 1; this ratio could be calculated from deformations based on some simpler model. The check of the deformed shape after being loaded by the corresponding blood pressure should be done by comparison with the CT scan made under the corresponding conditions.

The models of the SMCs are rather different from each other. *Model No. 2* (homogeneous) is as simple that its five Mooney-Rivlin constants can be identified unambiguously using tension test only. This model can simulate the mechanical properties of the SMC in a higher level structure (tissue) but it is not sufficient for understanding the tissue reaction on the load that must be induced at the level of its structural parts.

Model No. 3 represents our first attempt of creating a model of SMC taking the cell structure into account. As the number of unknown material parameters is too high, they were not identified but only chosen to give realistic results of the indentation test. Then the sensitivity analysis was made to estimate the influence of the stiffness (modulus of elasticity) of the individual parts on the simulation results.

It is evident that the resulting curves are mostly influenced by the stiffness of cytoplasm and microtubuli. In opposite to our assumptions, the influence of membrane skeleton was lower (but still significant), while the influence of nucleus and of microfilaments was negligible. The elasticity moduli of

ISSN: 1727-1983

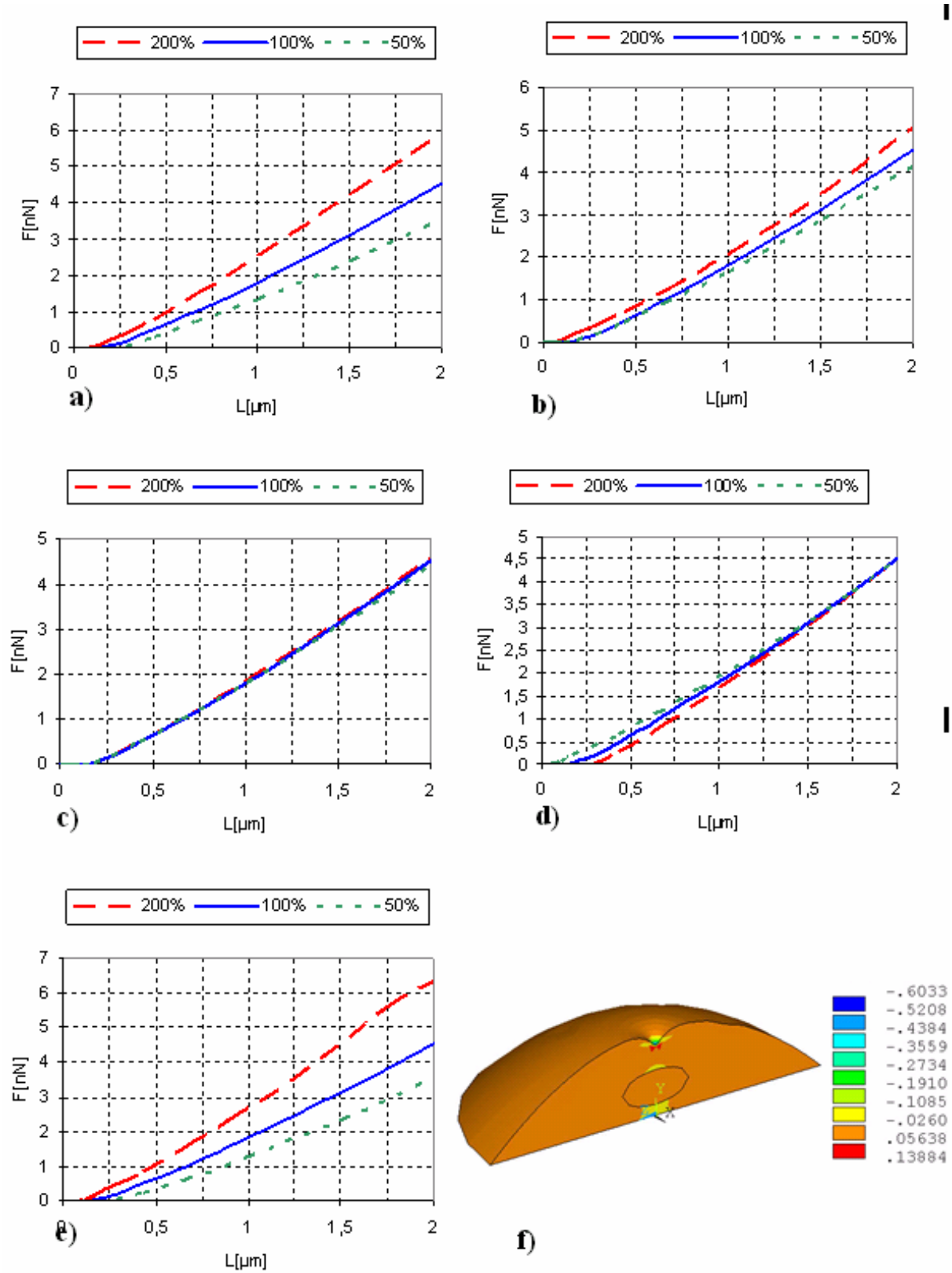

Fig.7: Influence of the individual cell model components on the resulting curves of computational simulation of indentation tests. The curves force F vs. indentation depth L present influences of the following changes in elasticity moduli of: a-cytoplasm, b-membrane skeleton, c-nucleus, d-microfilaments, e-microtubuli, all in the range from 50 (dotted lines) up to 200 % (dashed lines) of the nominal value (solid line). Fig. f) presents an illustrative distribution of the 1st principal stress [kPa] in the cytoplasm and nucleus.

ISSN: 1727-1983

struts and cables of the cytoskeleton, however, are extremely high; this discrepancy can be due to the too simple tensegrity structure. The real cytoskeleton structure is very complex and counts an excessive lot of basic elements, microtubuli and microfilaments (see e.g. [8], [9]). The cross sections of the struts and cables in the model were defined in accordance with the cross sections of the microtubuli and microfilaments, what results in their very high elasticity moduli. However, it has no effect to change the cross sections of the 1D elements, the only way to achieve better accordance with reality is to use a more complex tensegrity structure in the model what should be done in near future.

Conclusions

The computational *model No. 1* evaluates the stress states in the maximum diameter region of the AAA. The stress increase caused by the AAA is quantified by the maximum principal stress ratio between the AAA and the intact aorta. This ratio is influenced not only by the diameter of AAA, but also by the thickness of the arterial wall (or of its layers), thrombus effect, real irregular geometry of the AAA, and by material properties of individual tissues. Therefore it could enable us to judge the risk of AAA rupture much more effectively and exactly than by the mere monitoring of the maximal outer diameter how it is done in clinical practice.

The other two models represent computational simulation of various tests carried out with SMC. The model No.2 based on the homogeneous material properties of cytoplasm enables us to identify the elastic parameters of the material using the tension test only. This model can be sufficient for modelling the mechanical behaviour of the cell as a whole in a higher structure (tissue), but it cannot be sufficient for understanding tissue remodelation and other physiological or pathological processes being induced at the level of cell organelles. It requires a more complex model taking the organelles significant from the mechanical viewpoint into account; for the identification of material parameters of such a model, however, more tests with the particular type of cell should be carried out and simulated by computational modelling.

References

[1] HOLZAPFEL M., Sommer G., Regitnig P.(2004): 'Anisotropic mechanical properties of tissue components in human atherosclerotic plaques', *J. Biomechanical Engineering*, **126**, pp. 657-665

[2] SATO M. et al. (1987): 'Micropipette aspiration of cultured bovine aortic endothelial cells exposed to shear stress', *Arteriosclerosis*, **7**, 276-286

[3] HAYASHI K. (2004): 'Tensile properties and local stiffness of cells', Symposium IUTAM, Graz, Austria

[4] MIYAZAKI H., HASEGAWA Y., HAYASHI K. (2002): 'Tensile properties of contractile and synthetic vascular smooth muscle cells', *JSME Int. J.,* **45,** pp.870-879

[5] THOUMINE O., OTT A. (1997): 'Time scale dependent viscoelastic and contractile regimes in fibroblasts probed by microplate manipulation', *Journal of Cell Science*, **110**, pp. 2109-2116

[6] ROSS M.H. (2002): 'Histology, a text and atlas', (Williams and Wilkins)

[7] LEBIŠ R., BURŠA J., HAYASHI K. (2004): 'Constitutive model of vascular smooth muscle cells determined using computational simulation', Proc. Engineering Mechanics 2004, Svratka, CR, pp. 167-168

[8] SEOW C.Y., PRATUSEVICH V.R., FORD L.E. (2000): 'Series-to-parallel transition in the filament lattice of airway smooth muscle', *J.Appl. Physiol.*, **89**, pp. 869-876

[9] SMALL J.V., GIMONA M. (1998): 'The cytoskeleton of the vertebrate smooth muscle cell', *Acta Physiol. Scand.*, **164**, pp. 341-348

ISSN: 1727-1983